P4.3. APPLICATION OF WRF-BASED FORECASTS OF TOTAL LIGHTNING THREAT TO THE CONUS

Eugene W. McCaul, Jr.*, Universities Space Research Association, Huntsville, AL
Jonathan L. Case, ENSCO/NASA SPoRT Center, Huntsville, AL
Scott R. Dembek, USRA/CIMMS, Kennett Square, PA
Steven J. Goodman, NOAA/NESDIS, Silver Spring, MD

1. INTRODUCTION

With the upcoming launch of the Geostationary Lightning Mapper (GLM; Christian 2006), interest continues in exploring GLM proxy lightning data for diverse applications such as data assimilation into convection-allowing models, detection of lightning initiation and cessation, hurricane rapid intensification, and assessment of lightning-induced wildfire threat. Quantitatively calibrated proxy fields of lightning flash rate density for convection-allowing model output data were developed by McCaul et al. (2009), using a method based upon the findings of global satellite radar and lightning studies (Cecil et al. 2005; Petersen et al. 2005; Deierling and Petersen, 2008). In these studies, clear relationships were found between lightning flash rates seen by the Tropical Rainfall Measuring Mission (TRMM) Lightning Imaging Sensor and collocated large precipitating ice detected by the TRMM Precipitation Radar.

Based on these observational findings, two separate model proxy fields were examined by McCaul et al. (2009), one involving the upward flux of graupel at the -15°C level, the other simply the vertically integrated ice. For a limited but diverse sample of storm cases in the Huntsville, Alabama, area, for which ground-truth total lightning flash data from the North Alabama Lightning Mapping Array (NALMA, Goodman et al. 2005; Rison et al. 1999; Krehbiel et al. 2000) were available, the peak values of observed flash rate densities were found to correlate well with the peak values of the proxy fields simulated with the Weather Research and Forecasting (WRF; Skamarock et al. 2005) model. Scatterplots showed the observed data and proxy data bore an apparent linear relationship, with regressions passing near or through the origin.

McCaul et al. (2009) thus found that both proxies could be calibrated using simple proportionality factors to provide accurate estimates of lightning flash rate density. Both proxies also offer the advantage of providing guidance on lightning threat over much more limited areas than other traditional thunderstorm forecast metrics. However, each of the proxies had their own specific limitations. In particular, while the graupel flux proxy exhibited realistic temporal variability of lightning, it failed to describe lightning activity in storm anvils, while the ice integral proxy failed to exhibit proper temporal variability but, with appropriate thresholding, could provide accurate areal coverage of the overall lightning threat. Thus, a viable solution for fully describing the amplitude, variability, and areal coverage of lightning threat was a weighted-average blending of the two proxy threats. To retain as much of the temporal variability as possible, a weighting of 0.95 was used for the graupel flux threat, while the remaining 0.05 weighting for the ice integral threat was found to be sufficient to retain good areal coverage in the blended product.

Because the original McCaul et al. (2009) study used WRF model data from a 2-km native grid mesh, with a specific set of model physical and microphysical parameterization choices, including WRF Single Moment 6-Species (WSM6) microphysics, it was important to extend the study to other WRF configurations and additional storm case scenarios to examine algorithm robustness. In this paper, we document preliminary findings from such studies, suggest tentative changes to the algorithm, and provide results from additional Continental U.S.-wide applications of the modified algorithm using the daily WRF runs executed by the National Severe Storms Laboratory (NSSL) in 2010. Expanded future plans for algorithm testing are also described.

2. METHODOLOGY

The McCaul et al. (2009 WRF Lightning Forecast Algorithm (LFA) described above was installed in the source code of the NSSL WRF model in February 2010, in time for use in the Hazardous Weather Testbed (HWT) 2010 Experiment Forecast Program (EFP). Because the NSSL WRF data are saved and displayed only once every hour of simulated time, it was necessary to build fields of the cumulative hourly maxima of both the graupel flux threat (referred to as Threat 1) and vertically integrated ice threat (referred to as Threat 2) for optimum accuracy. This was accomplished using the methods described by Kain et al. (2010). Use of only hourly snapshot data would likely have caused the true peaks in the fields contributing to the two lightning threats to be missed, and these peaks are believed to be the best basis for comparison with observational data. For simplicity, the blended threat (referred to as Threat 3) was computed using only the hourly cumulative peaks of the graupel flux and ice integral threats.

Fields of the cumulative values of Threats 1, 2, and 3 were computed within the model during execution, because of the need to construct the cumulative

*Corresponding author address: E. W. McCaul, Jr., Universities Space Research Association, 6767 Old Madison Pike, Suite 450, Huntsville, AL 35806, e-mail: emccaul@usra.edu

fields of Threats 1 and 2. In assessing Threat 3, values of Threat 1 were rescaled such that their peaks matched those of Threat 2, because of preliminary findings from 2008 EFP cases that showed that the values of Threat 1 might be systematically too small. The underperformance of Threat 1 apparently derived from the predominance of weaker updrafts on the NSSL WRF 4-km mesh, which was twice as coarse as the 2-km mesh used in the McCaul et al.(2009) study. In the installation of the algorithm into the NSSL WRF, no allowances were made for variations in the choices of physical parameterizations used. Preliminary tests made on convective ensemble data generated by the Center for Analysis and Prediction of Storms (CAPS) in 2008 suggested these sensitivities were, on average, smaller than those associated with the grid mesh spacing.

Once the NSSL WRF runs featuring LFA output began to be published (see www.nssl.noaa.gov/wrf), the LFA output fields were monitored frequently to study algorithm performance. A database of peak values of the various lightning threat fields from a range of important and interesting cases was developed. Plans are for the data to be scrutinized in detail in the near future, but a few salient preliminary observations are made below.

3. RESULTS AND DISCUSSION

Overall, the quantitative fields from the LFA, as implemented in the NSSL WRF, appeared reasonable and useful (Miller et al. 2010). There were several instances of cold season precipitation events which contained enough vertically integrated ice to trigger Threat 2, even in the absence of any graupel flux from Threat 1. Active convective events behaved as expected, for the most part, even for several very damaging supercell tornado outbreaks. The only areas of concern were related to a few very high flash rate events, as described later.

On 24 April 2010, numerous tornadic supercells swept across the Deep South, with Mississippi and Alabama receiving the most casualties and damage. Some of the most destructive of these storms occurred across north central Alabama after 00 UTC 25 April 2010, and were detected by NALMA. Based on the NSSL WRF forecast, peak values of lightning Threat 1 were estimated to be 16.2 fl km $^{-2}$(5 min)$^{-1}$ in southern Middle Tennessee at 22 UTC 24 April (see Fig. 1). The actual peak observed flash rate density detected by NALMA (not shown) was 18.1 fl km $^{-2}$(5 min)$^{-1}$, in good agreement with the WRF forecast value. The timing and location of the forecast maximum lightning threat was not, however, coincident with the observed peak, which occurred at 0435 UTC 25 April in northeast Alabama.

Another major event occurred on 10 May 2010 in Oklahoma and Kansas, during a damaging supercell tornado outbreak within the surveillance area of the Oklahoma LMA (OKLMA). WRF forecasts for this event showed peak values of Threat 1 of about 11.6 fl km $^{-2}$(5 min)$^{-1}$ after 03 UTC 11 May, with Threat 2 only slightly smaller at 10.9 fl km $^{-2}$(5 min)$^{-1}$ (Fig. 2). OKLMA analyses of lightning observations (not shown) will be conducted in the near future. For both this case and the 24 April 2010 case, the WRF peak threat values were moderately intense, but not very much larger than the intense storm cases studied during LFA construction by McCaul et al. (2009).

Of greater overall concern during Spring-Summer 2010 was the occurrence of a few very high flash rate storm events that featured unexpectedly large values of Threat 1, based on large updraft speeds and sizable graupel mixing ratios in the -15°C layer. The largest value of Threat 1 documented informally was 30.9 fl km $^{-2}$(5 min)$^{-1}$. This event occurred at 22 UTC 17 July 2010 in northeastern South Dakota (see Fig. 3), an area which is not covered by any LMA network. Updraft speeds on the WRF 4-km mesh reached 39.3 m s^{-1}, perhaps not surprising in light of the convective available potential energy (CAPE) values exceeding 6000 J kg^{-1}in the upper Mississippi Valley area on that afternoon (not shown). These very large Threat 1 values were accompanied by Threat 2 values that reached only 18.1 fl km $^{-2}$(5 min)$^{-1}$.

Several other cases of extreme values of Threat 1 were also found in areas covered by the OKLMA and NALMA networks. At 23 UTC 2 June 2010, an instance of Threat 1 reaching a peak of 28.9 fl km $^{-2}$(5 min)$^{-1}$ was noted from a storm in north Texas (not shown). Threat 2 showed a peak of only 16.2 fl km $^{-2}$(5 min)$^{-1}$ for this storm. In the Tennessee Valley area, a storm at 04 UTC on 5 August 2010 (not shown) generated a peak Threat 1 value of 25.3 fl km $^{-2}$(5 min)$^{-1}$, accompanied by a Threat 2 value of 16.3 fl km $^{-2}$(5 min)$^{-1}$.

The values of LFA-diagnosed lightning flash rate density in these latter three cases are well above the largest values found in the Tennessee Valley training dataset which was used to develop the LFA. More importantly, the Threat 1 values in these cases exhibit an obvious tendency to exceed Threat 2, sometimes by a large margin (see Fig. 4). The divergence of Threat 1 and Threat 2 values for the highest flash rate storms suggests nonlinear behaviors in the calibration curves for one or both threats at very high flash rates. One hypothesis is that there is a practical upper limit to the values produced by Threat 2, owing to practical upper limits on values of precipitable water feeding these intense storms. It is postulated that there is little net increase in vertically integrated ice as ambient precipitable water values reach near climatological extremes. However, values of CAPE, an important predictor of storm peak updraft speeds, are very sensitive to slight changes in moisture at extreme values of lower tropospheric water vapor mixing ratio. As a consequence, updraft speeds can become very large and boost values of Threat 1, even while values of Threat 2 become limited by the climatological ceiling in values of precipitable water. To test this hypothesis, there is a need to incorporate some of these extreme flash-rate storms

into the LFA database and revisit the calibration procedure, using observations from OKLMA and NALMA. Pursuit of this work is in the planning stages.

4. SUMMARY AND OUTLOOK

The results from daily use of the LFA in the NSSL WRF forecasts from 2010 are encouraging, but indicate that further refinements of the algorithm are needed to improve robustness for very high flash rate storms. It is possible that exploration of the calibrations of the LFA proxies at very high flash rates will find that nonlinearities are present for one or both of the LFA lightning threat variables.

Plans are underway to examine in more detail the high flash rate cases already mentioned from the NSSL 2010 forecast archive, to evaluate the actual total flash rates as seen by the relevant LMA networks. This will allow extension of the calibration curves into the high flash rate portion of the parameter space, and suggest ways to improve the calibration of the algorithm.

Plans are also underway to install the WRF LFA into the WRF ensemble members to be executed by CAPS during upcoming HWT EFPs. This will provide a wealth of additional cases for potential inclusion in expanded LFA calibration studies. This will also provide insight into the sensitivity of LFA output to variations in model physics and initial conditions, information needed by the data assimilation community as consideration is given to assimilating real data collected by the GLM in the future.

5. ACKNOWLEDGMENTS

This work was supported by NASA's Short-term Prediction and Research Transition (SPoRT) Center in Huntsville, AL, with additional support from the GOES-R Risk Rediction Research Program. Special thanks go to Gary Jedlovec, Bill Koshak, and Rich Blakeslee, NASA Marshall Space Flight Center, Huntsville, AL, for their support of this research.

6. REFERENCES

Cecil, D. J., S. J. Goodman, D. J. Boccippio, E. J. Zipser, and S. W. Nesbitt, 2005: Three years of TRMM precipitation features. Part I: Radar, radiometric, and lightning characteristics. *Mon. Wea. Rev.*, **133**, 543–566.

Christian, H. J., 2006: Geostationary Lightning Mapper (GLM). 2nd Conf. Meteorol. Appl. Lightning Data, Atlanta, Amer. Meteorol. Soc., Paper J2.3.

Deierling, W., and W. A. Petersen, 2008: Total lightning activity as an indicator of updraft characteristics. *J. Geophys. Res.*, **113**, D16210, doi:10.1029/2007JD009598

Goodman, S. J., R. Blakeslee, H. Christian, W. Koshak, J. Bailey, J. Hall, E. McCaul, D. Buechler, C. Darden, J. Burks, T. Bradshaw, and P. Gatlin, 2005: The North Alabama Lightning Mapping Array: Recent severe storm observations and future prospects. *Atmos. Res.*, **76**, 423–437.

Kain, J. S., S. R. Dembek, S. J. Weiss, J. L. Case, J. J. Levitt, and R. A. Sobash, 2010: Extracting unique information from high-resolution forecast models: Monitoring selected fields and phenomena every time step. *Wea. Forecasting*, **25**, 1536–1542.

Krehbiel, P.R., R.J. Thomas, W. Rison, T. Hamlin, J. Harlin, and M. Davis, 2000: GPS-based mapping system reveals lightning inside storms. EOS, **81**, 21-25.

McCaul, E. W., Jr., S. J. Goodman, K. M. LaCasse, and D. J. Cecil, 2009: Forecasting lightning threat using cloud-resolving model simulations. *Wea. Forecasting*, **24**, 709–729. (highlighted as a Paper of Note in *Bull. Amer. Meteorol. Soc.*, **90**, 772.)

Miller, S. D., Jr., G. W. Carbin, J. S. Kain, E. W. McCaul Jr., A. R. Dean, C. J. Melick, and S. J. Weiss, 2010: Preliminary investigation into lightning hazard prediction from high-resolution model output. 25th Conf. Severe Local Storms, Denver, CO, Amer. Meteor. Soc., Paper B4.1.

Petersen, W. A., H. J. Christian, and S. A. Rutledge, 2005: TRMM observations of the global relationship between ice water content and lightning. Geophys. Res. Lett., **32**, L14819, doi: 10.1029/2005GL023236.

Rison, W., R. J. Thomas, P. R. Krehbiel, T. Hamlin, and J. Harlin, 1999: A GPS-based three-dimensional lightning mapping system: Initial observations in central New Mexico. Geophys. Res. Lett., **26**, 3573-3576.

Skamarock, W. C., J. B. Klemp, J. Dudhia, D. O. Gill, D. M. Barker, W. Wang, and J. G. Powers, 2005: A description of the Advanced Research WRF Version 2. NCAR Technical Note NCAR/TN-468+STR, 100 pp.

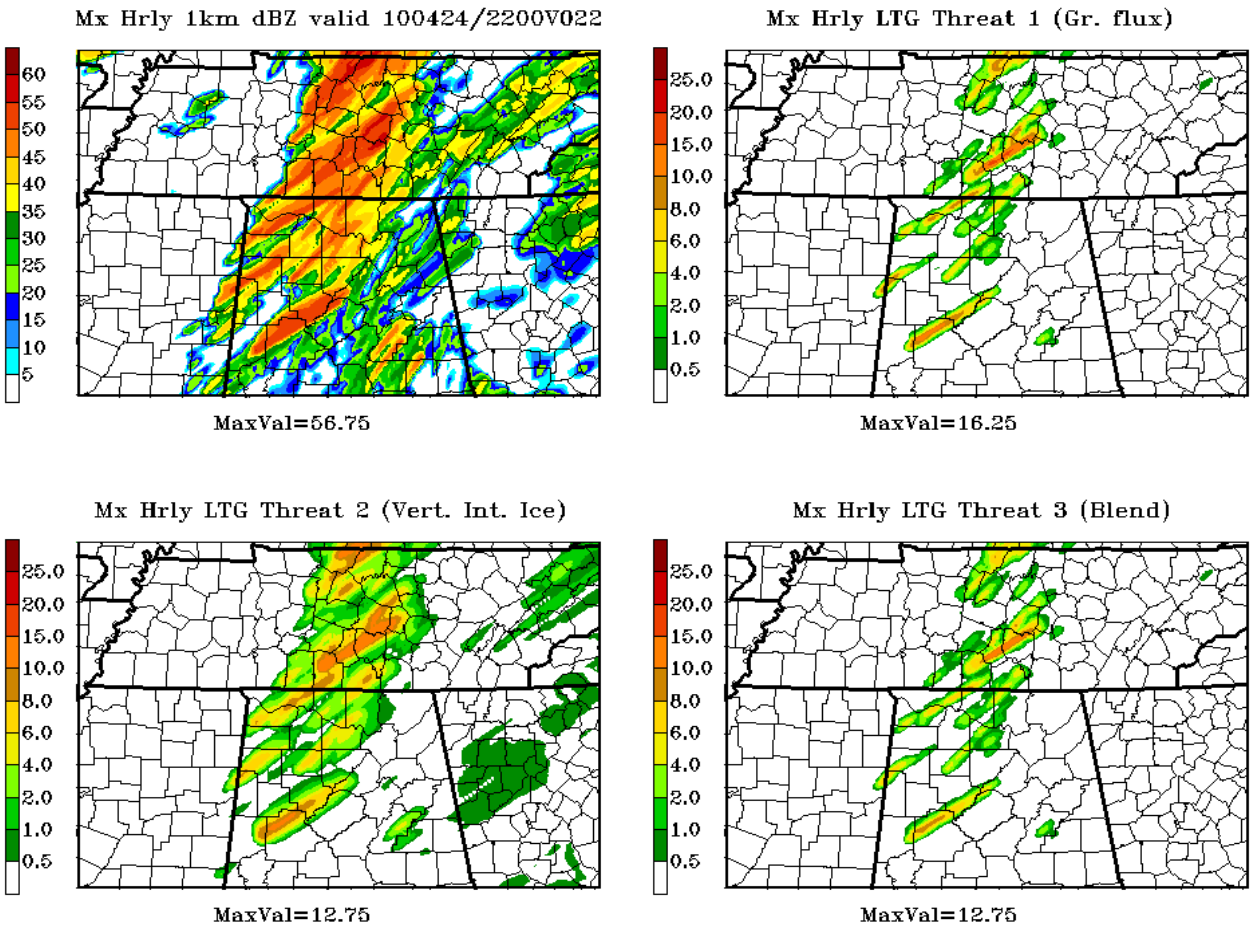

Fig. 1. Fields of maximum hourly values of 1-km reflectivity (upper left panel), Lightning Threat 1 based on graupel flux (upper right), Lightning Threat 2 based on vertically integrated ice (lower left), and Blended Lightning Threat (lower right), from NSSL WRF forecast for 22 UTC 24 April 2010 within the North Alabama region. Regional maximum values of each field (dBZ for reflectivity, fl km $^{-2}$ (5 min)$^{-1}$ for each lightning threat) are printed beneath each panel for easy reference.

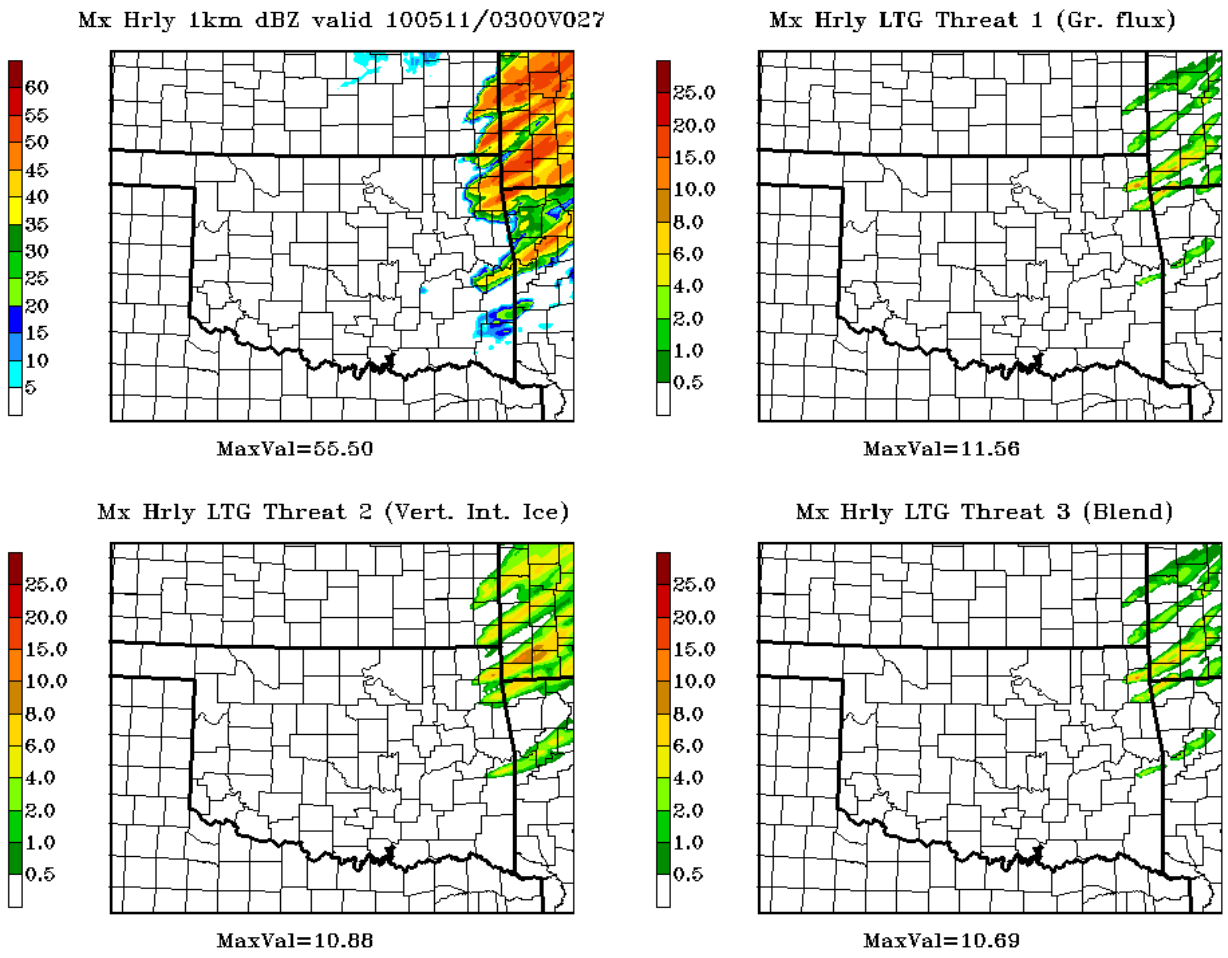

Fig. 2. As in Fig. 1, but for 03 UTC 11 May 2010 in the Oklahoma region.

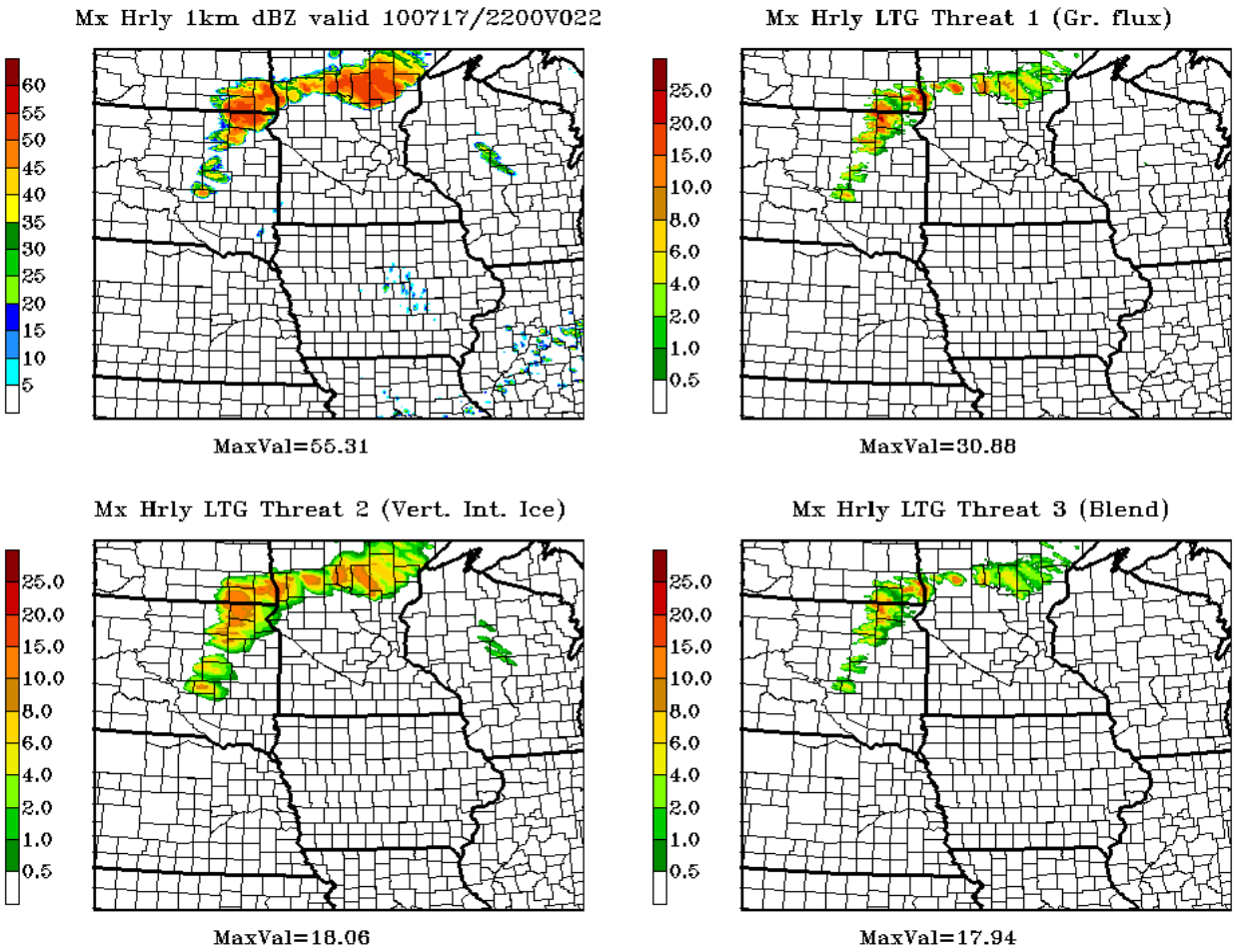

Fig. 3. As in Fig. 1, but for 22 UTC 17 July 2010 in the Upper Mississippi Valley.

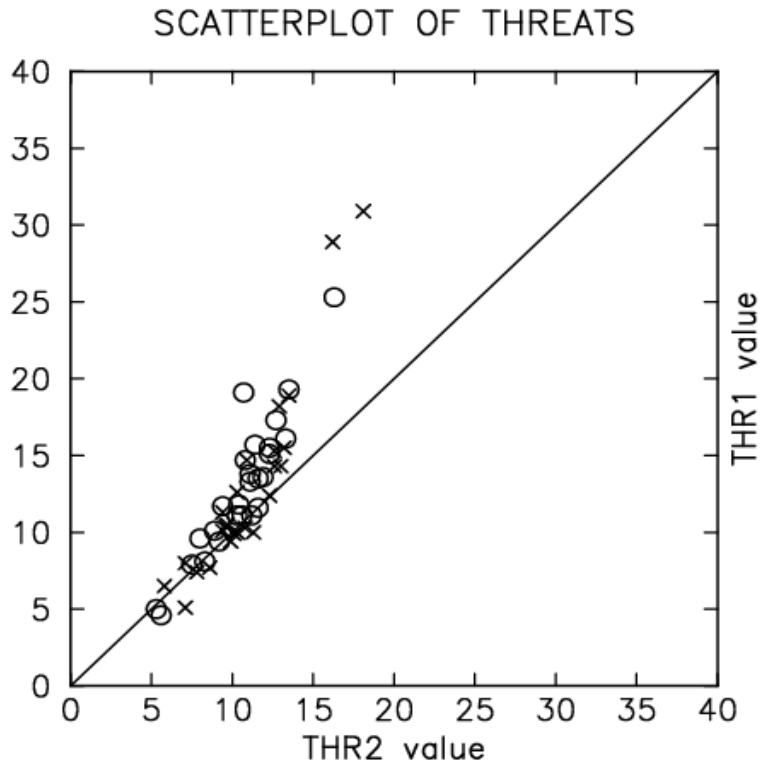

Fig. 4. Scatterplot of peak values of Lightning Threat 1 (ordinate) vs. Lightning Threat 2 (abscissa). Note the deviation of points away from the diagonal at very large threat values, suggestive of calibration errors for storms with extremely intense lightning.